Applied Mathematics & Information Sciences
An International Journal

http://dx.doi.org/10.18576/amis/100227

Effect of Partial Slip on Peristaltic Flow of a Sisko Fluid with Mild Stenosis through a Porous Medium

Nabil T. M. El-dabe, Galal M. Moatimid, Mohamed A. Hassan and Doaa R. Mostapha *

Department of Mathematics, Faculty of Education, Ain Shams University, Roxy, Cairo, Egypt.

Received: 24 Aug. 2015, Revised: 11 Nov. 2015, Accepted: 12 Nov. 2015
Published online: 1 Mar. 2016

Abstract: This paper investigates the effect of partial slip on peristaltic flow of a Sisko fluid through a porous medium. The flow is streaming through a tapered artery having a mild stenosis. The influences of heat and chemical reactions on blood flow are also taken into account. The governing equations of motion, energy and concentration are simplified by using the long wavelength and low Reynolds number approximations. The analytical solutions of these equations are obtained by considering a perturbation technique for small non-Newtonian Sisko fluid parameter. The pressure rise and friction force are numerically calculated. The numerical calculations with the help of graphs are adopted to obtain the effects of several parameters, such as the slip parameter, permeability parameter, the taper angle, Brickmann number, Soret number and the maximum height of stenosis, upon the distributions of velocity, temperature, concentration, pressure rise and friction force. It is found that the axial velocity increases with the increase of slip parameter. Meanwhile, it decreases with the increase of permeability parameter. The stream lines are also depicted. It is observed that the trapped bolus increases in size with the increase of both the slip parameter and the maximum height of stenosis. The other results are also illustrated.

Keywords: Peristaltic flow; Sisko model; Tapered artery; Stenosis flow; Porous medium; Slip flow; Heat transfer; Trapping phenomena.

1 Introduction

Several researches studied the non-Newtonian fluids because of their importance in industrial and technological applications. Sisko [1] proposed a new model in studying the non-Newtonian fluid, which is later called sisko fluid. Sisko fluid is a model which combines the features of viscous and generalized of power law models. It is capable of describing shear thinning and thickening phenomena, which commonly exist in nature. It has many industrial applications such as waterborne coatings, metallic automotive, cement slurries, lubricating greases, psueodo-plastic fluids and drilling fluids. Sisko fluid is an example of viscoelastic materials that include polymeric liquids, biological fluids, liquid crystals, lubricating oils, mud and paints [2]. It can demonstrate many typical characteristics of Newtonian and non-Newtonian fluids by choosing different material parameters. Therefore, we may considered it as a blood model.

Peristaltic transport is produced by a traveling wave of area contraction and expansion along the wall of the tubes. It occurs generally from a region of lower pressure to higher pressure. It is very important in biological mechanism which responsible for various physiological functions of the organs of the human body. It has many applications [3], such as transport deionized water and whole blood and deliver phosphated buffered saline into the vein of a rat, the transport of urine from kidney to bladder, transport of food through oesophagus, the movement of eggs in the fallopian tube, transport of the spermatozoa in the cervical canal, transport of blood in heart, transport of bile in the bile duct. Several theoretical

* Corresponding author e-mail: dodyyasser017@yahoo.com

and experimental articles have been examined the peristaltic flows, such as Shapiro [4], Manton [5] and Fung and Yih [7]. Their works considered several assumptions, such as long wavelength approximation, low Reynolds number, small wave number and small amplitude ratio. The peristaltic transport through infinitely long symmetric channel or axi-symmetric tubes containing a Newtonian or non-Newtonian fluids have been investigated. Asif et al. [8] studied the problem of peristaltic transport of a non-Newtonian power law fluid characterized by the streaming blood through an axi-symmetric tapered tubular vessel under a long wave length approximation.

Blood is a mixture of of red cells, white cells and platelets in plasma. The analysis of blood flow through stenosed arteries is very important. The discovery of the cardiovascular diseases, such as stenosis or arteriosclerosis, is closely associated with the flow conditions in the blood vessels. A stenosis is the abnormal growth of tissue. Stenosis means narrowing of any body passage [9]. stenoses may be caused by the impingement of extra vascular masses. Also, it may be formed due to intravascular atherosclerotic plaques which develop at the wall of the artery and protrude into the lumen. It may leads to cerebral strokes, myocardial infarction and heart failure by reducing or occluding the blood supply [10]. Also, in case of stenosed artery, stresses and resistance flow are higher than those in case of the normal ones. Furthermore, stenosis may damage the internal cells of the wall. Several efforts have been made to investigate the blood flow characteristics through stenosed arteries. Chakravarty et al. [11] investigated the problem of nonlinear blood flow in a stenosed flexible artery. Also, Verma and Parihar [12] discussed the mathematical model of blood flow through a tapered artery with mild stenosis.

Heat transfer analysis is one of the important topic in studying chemical engineering. It has a great importance in the peristaltic motion. It is the passage of thermal energy from a hot body to a colder one. Bio-heat is considered as heat transfer in human body. It includes thermotherapy and human thermoregulation system [13]. The thermotherapy system is on of the most important application of heat in the human body. The human thermoregulation system is the ability of living body to maintain temperature with in certain limits in case of surrounding temperature variations. In physiology, it is used to study the properties of tissues. Heat transfer analysis is important especially in case of non-Newtonian peristaltic rheology. It is used in many complicated processes in the human body. Heat transfer is used in perfusion of the arterial venous blood through the pores of the tissue (process of delivery of blood to capillary bed). Furthermore, it used to generate metabolic heat and heat transfer due to some external interactions such as, mobile phones and radioactive treatments. The application radio-frequency therapy is important to treat more diseases such as tissue coagulation, the primary liver cancer, the lung cancer and the reflux of stomach acid [14]. Many investigators have reported the influence of heat transfer on peristaltic flow of Newtonian and non-Newtonian fluids, see [15].

In the recent past, many researches investigated, theoretically and experimentally, the combined effects of heat and mass transfer on bio-fluids [16]. The quantitative prediction of blood flow rate and heat generation are important for diagnosing blood circulation illness. Also, the combining between heat and mass transfer is important for the noninvasive measurement of blood glucose [17]. The mass flux caused by the temperature gradient, which is called Soret effect or thermal-diffusion, is discussed by Alam et al. [18]. The Soret effect is often negligible in heat and mass transfer processes due to its small order of magnitude. However, for the non-Newtonian fluids with light or medium molecular weight, it is not appropriate to neglect Soret effect as studied by Dursunkaya and Worek [19]. Therefore, through this study, we investigate the combined effects of heat and mass transfer with Soret effect. Nadeem and Akbar [20] studied the effect of heat and mass transfer on Walter's B fluid through a tapered artery. Also, the problem of dynamic response of heat and mass transfer in blood flow through stenosed arteries has been discussed by Chakravarty and Sen [21].

The effect of vessel tapering is an important factor in studying peristaltic transport. Pandey and Chaube [22] studied the axi-symmetric peristaltic transport of a viscous incompressible viscoelastic fluid through a circular tube whose cross section changes along the length (tapered tube). The Newtonian and non-Newtonian blood flow through tapered arteries with a stenosis have been investigated. Mandal [23] studied the notable characteristics of the non-Newtonian blood flow (Power-law model) through a flexible tapered arteries in the presence of stenosis subject to the pulsatile pressure gradient. Also, Mekheimer and El Kot [24] investigated the influence of heat and chemical reactions of blood flow through tapered artery with stenosis. They considered a Sisko fluid as a model of blood. They obtained that the magnitude of axial velocity is greater for a Newtonian fluid than that for a Sisko fluid. Also, the curves through

the convergent tapered artery are greater than those in the non tapered artery and the diverging tapered artery.

Porous media play an important role in many branches of engineering, including material science, petroleum industry, chemical engineering, and soil mechanics as well as biomechanics. The flow through porous media has gained a considerable interest during recent years, particularly among geophysical fluid dynamicists. It occurs in filtration of fluids in heat pipes and seepage of water in river beds. There are some important examples of flow through porous medium such as solid matrix heat exchangers, electronic cooling chemical reactors, sandstone, limestone, movement of underground, water, oils, rye bread, bile duct, wood, the human lung, gall bladder with stones and small blood vessels. Also, the seepage under a dam is an important application through the porous media. An excellent review in the physics of porous media is given by Scheidegger [25] and Eldabe [26]. Mekheimer [27] studied the motion of an incompressible, viscous fluid in an inclined planar channel filled with a homogenous porous medium and having walls that are transversely displaced by an infinite, harmonic traveling wave of large wavelength. This problem was analyzed using a perturbation expansion in terms of a variant wave number. Mekheimer obtained an explicit form for the velocity field and a relation between the pressure rise and flow rate in terms of Reynolds number, wave number, permeability parameter, inclined angle, and the occlusion. Also, Afsar et al. [28] discussed the problem of peristaltic flow of a Jeffrey fluid with variable viscosity through a porous medium in an asymmetric channel. It is observed that the magnitude of axial velocity decreases with the increasing of the permeability parameter.

In studying the peristaltic flow, many researches assumed that the fluid layer next to the surface moves with it, which is so called no slip condition. However, there are another works that considered hypotheses including slippage. The so called slip conditions means that there is a relative motion between the fluid layer next to the fluid surface. It states that the velocity of the fluid at the plate is linearly proportional to the shear stress at this plate. It is very important in the polishing of artificial heart valves. Also, it is important for internal cavities in a variety of manufactured parts, micro-channels or nano-channels. The slip condition plays a vital role in shear skin spurt and hysteresis effects. Furthermore, the fluids that exhibit boundary slip have essential technological applications when a thin film of light oil is attached to the moving plates. Also, it is used when the surface is coated with a special coating such as a thick monolayer [29]. The problem of effects of magnetic field and wall slip conditions on the peristaltic transport of a newtonian fluid in an asymmetric channel is discussed by Ebaid [30]. Also, Mekheimer et al. [31] investigated the effects of slip condition and porous medium on peristaltically induced MHD due to a surface acoustic wavy wall.

In the last decades, a growing interest [[24] and [31]] deals with studying the chemical reaction, slip or no slip conditions in Newtonian as well as the non- Newtonian fluids. This is because of their great importance in several areas such as medicine and medical industries. Therefore, the aim of the present study focus on investigating the effects of heat and chemical reactions on peristaltic transport of blood flow. The flow is streaming through a tapered artery with mild stenosis. The blood is represented by a Sisko model. Furthermore, the influences of slip condition and porous medium are also considered. The governing equations of motion, energy and concentration are simplified using the long wavelength and low Reynolds number approximation. These equations are analytically solved in accordance with the appropriate boundary conditions. The technique depends on a perturbation analysis. This technique considers a small Sisko fluid parameter. The distributions of the stream function, temperature and concentration are obtained up to the first order. The pressure rise and friction force are obtained in terms of dimensionless flow rate Q by using numerical integration. Numerical calculations are adopted to obtain the effects of several parameters, such as the slip parameter, permeability parameter, the taper angle, Brickmann number, Soret number and the maximum height of stenosis, on the above distributions. To clarify the problem at hand, in Section 2, the physical description of the problem including the basic equations governing the motion with the appropriate boundary conditions is presented. Section 3 is devoted to introduce the method of solution according to a perturbation technique. Through Section 4, we introduce some important results that are displayed graphically for pumping characteristics and trapping phenomena. Finally, in Section 5, we give concluding remarks for this study based on the obtained results for peristaltic transport and stream lines.

2 Formulation of the problem

Consider an unsteady motion of Sisko fluid through a tapered tube with mild stenosis. The surface of the tube

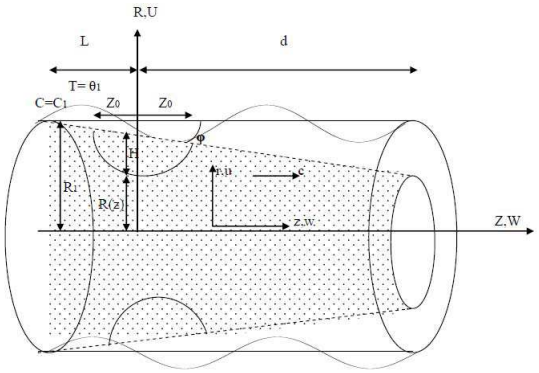

Fig. 1: Sketch of the physical situation of the problem.

has an infinite sinusoidal wave train traveling along the axis of the tube. The flow is streaming through a porous medium. Cylindrical polar co-ordinates system (R, θ, Z) is used, so that the Z-axis coincides with the axis of the tube. Through this study, an axial symmetry is considered. In other words, all physical quantities are independent on the coordinate θ. The stenosis is developed in an axially symmetric manner. Heat and mass transfer are also taken into account. The wall of the tube is maintained at the uniform temperature θ_1 and concentration C_1, respectively. Meanwhile, at the centre of the tube we consider the symmetry conditions on both temperature and concentration. The slip condition is also considered.

The effective radius of the tube [12] is taken as follows:

$$R(z)=\begin{cases} R_1-m\delta(z+L) & L<z<-z_0, \\ R_1-m\delta(z+L)-\frac{H}{2}[1+\cos\frac{\pi z}{z_0}] & -z_0\le z\le z_0, \\ R_1-m\delta(z+L) & z_0<z<d, \end{cases} \tag{1}$$

where $R(z)$ is the effective radius of the tapered artery, R_1 is the radius of the un-tapered artery, $\delta=\frac{R_1}{\lambda}$, λ is the wave length, $H=h\cos\phi$ is the hight of the stenosis in the tapered artery, ϕ is the angle of tapering, h is the maximum hight of the stenosis, z_0 is the half-length of the stenosis and $m=\tan\phi$ is the slope of the tapered vessel. Sketch of the problem is given in the figure 1.

The ratio between the height of the stenosis and the radius of the normal artery is much less than unity. The arterial is taken to be of finite length $L+d$ [11]. This study focus on all possibilities of different shapes of the artery viz, the converging tapering $\phi<0$, non-tapered artery $\phi=0$ and the diverging tapering $\phi>0$ [23].

The prototype of fluid designed by Sisko is considered. Therefore, the constitutive equation is then become [2]

$$\underline{\mathbf{S}}=\left(a_1+b_1(\sqrt{\Theta})^{n-1}\right)\underline{\mathbf{A}}, \tag{2}$$

where $\underline{S}$ is the stress deviator, $\Theta=\frac{1}{2}tr(\underline{\mathbf{A}})^2$, $tr(\underline{\mathbf{A}})^2$ is the sum of elements in main diagonal of $(\underline{\mathbf{A}})^2$, n is the power index, a_1, b_1 are the material constant for Sisko fluid,

$$\underline{\mathbf{A}}=\mathbf{L}+\mathbf{L}^T \tag{3}$$

is the rate of strain tensor, $\underline{\mathbf{V}}=(U,0,W)$ is the velocity field and $\mathbf{L}=\nabla\underline{\mathbf{V}}$.

Since we assume that the fluid density ρ is uniform, it follows that the incompressibility condition (continuity equation) is then become

$$\nabla.\underline{\mathbf{V}}=0. \tag{4}$$

The equation of motion is

$$\rho\left(\frac{\partial\underline{\mathbf{V}}}{\partial t}+(\underline{\mathbf{V}}.\nabla)\underline{\mathbf{V}}\right)=-\nabla\Pi+\nabla.\underline{\mathbf{S}}-\frac{\eta}{p}\underline{\mathbf{V}}, \tag{5}$$

where Π is the pressure, η is dynamic viscosity and p is the permeability parameter.

The equation of energy [13] is

$$\rho c_p\left(\frac{\partial T}{\partial t}+\underline{\mathbf{V}}.\nabla T\right)=\Phi_1+K\nabla^2T, \tag{6}$$

where T is the temperature, $k=\frac{K}{\rho c_p}$ is the thermometric conductivity, K is the thermal conductivity, c_p is the specific heat and $\Phi_1=S_{ij}\frac{\partial V_i}{\partial X_j}$ is the dissipation term.

The equation of concentration is [17]

$$\frac{\partial C}{\partial t}+\underline{\mathbf{V}}.\nabla C=D\nabla^2C+\frac{DK_T}{T_m}\nabla^2T, \tag{7}$$

where C is the concentration distribution, D is the coefficient of thermal diffusivity, K_T is the thermal diffusion and T_m is the mean fluid temperature.

The geometry of the peristaltic wall surface is defined as [7]

$$h_1=a\cos\frac{2\pi}{\lambda}\left(Z-\frac{kt}{R_1}\right), \tag{8}$$

where a is the wave amplitude, λ is the wave length and $\frac{kt}{R_1}$ is the wave speed.

The appropriate boundary conditions may be listed as follows:

$$U=\frac{\partial h_1}{\partial t}, W=-\gamma S_{RZ}, T=\theta_1, C=C_1\,at\,R=R_2=R(z)+h_1, \tag{9}$$

$$U=0, \frac{\partial W}{\partial R}=0, \frac{\partial T}{\partial R}=0, \frac{\partial C}{\partial R}=0\,at\,R=0, \tag{10}$$

where γ is the slip parameter.

Combining Eqs. (2) and (3), the r and z-components the Eq. of motion (5) may be written as follows:
r-component:

$$\rho\left(\frac{\partial U}{\partial t}+U\frac{\partial U}{\partial R}+W\frac{\partial U}{\partial Z}\right)=-\frac{\partial \Pi}{\partial R}+\frac{2}{R}\left(a_1+b_1(\sqrt{\Theta})^{n-1}\right)\frac{\partial U}{\partial R}$$
$$+2\frac{\partial}{\partial R}\left(a_1+b_1(\sqrt{\Theta})^{n-1}\right)\frac{\partial U}{\partial R}+2\frac{\partial}{\partial Z}\left(a_1+b_1(\sqrt{\Theta})^{n-1}\right)$$
$$\left(\frac{\partial W}{\partial R}+\frac{\partial U}{\partial Z}\right)-\frac{2U}{R^2}\left(a_1+b_1(\sqrt{\Theta})^{n-1}\right)-\frac{\eta}{p}U, \tag{11}$$

and z-component:

$$\rho\left(\frac{\partial W}{\partial t}+U\frac{\partial W}{\partial R}+W\frac{\partial W}{\partial Z}\right)=-\frac{\partial \Pi}{\partial Z}+\frac{1}{R}\left(a_1+b_1(\sqrt{\Theta})^{n-1}\right)$$
$$\left(\frac{\partial W}{\partial R}+\frac{\partial U}{\partial Z}\right)+\frac{\partial}{\partial R}\left(a_1+b_1(\sqrt{\Theta})^{n-1}\right)\left(\frac{\partial W}{\partial R}+\frac{\partial U}{\partial Z}\right)$$
$$+2\frac{\partial}{\partial Z}\left(a_1+b_1(\sqrt{\Theta})^{n-1}\right)\frac{\partial W}{\partial z}-\frac{\eta}{p}W, \tag{12}$$

where $\Theta=2(\frac{\partial U}{\partial R})^2+2\frac{U^2}{R^2}+2(\frac{\partial W}{\partial Z})^2+(\frac{\partial U}{\partial Z}+\frac{\partial W}{\partial R})^2$.
With the continuity equation

$$\frac{1}{R}\frac{\partial (RU)}{\partial R}+\frac{\partial W}{\partial Z}=0. \tag{13}$$

The Eq. of energy (6) may be written as follows:

$$\rho c_p\left(\frac{\partial T}{\partial t}+U\frac{\partial T}{\partial R}+W\frac{\partial T}{\partial Z}\right)=\left(a_1+b_1(\sqrt{\Theta})^{n-1}\right)$$
$$\left(2(\frac{\partial U}{\partial R})^2+2(\frac{\partial W}{\partial Z})^2+(\frac{\partial U}{\partial Z}+\frac{\partial W}{\partial R})^2\right)$$
$$+K\left(\frac{\partial^2 T}{\partial R^2}+\frac{1}{R}\frac{\partial T}{\partial R}+\frac{\partial^2 T}{\partial Z^2}\right), \tag{14}$$

Also, the Eq. of concentration distribution (7) may be written as follows:

$$\frac{\partial C}{\partial t}+U\frac{\partial C}{\partial R}+W\frac{\partial C}{\partial Z}=D\left(\frac{\partial^2 C}{\partial R^2}+\frac{1}{R}\frac{\partial C}{\partial R}+\frac{\partial^2 C}{\partial Z^2}\right)$$
$$+\frac{DK_T}{T_m}\left(\frac{\partial^2 T}{\partial R^2}+\frac{1}{R}\frac{\partial T}{\partial R}+\frac{\partial^2 T}{\partial Z^2}\right). \tag{15}$$

The instantaneous volume flow rate in the fixed coordinate system is defined as:

$$Q=2\pi\int_0^{R_2} WRdR, \tag{16}$$

where R_2 is a function of Z and t.
The time averaged $\hat{Q}$ (time mean flow) over period $\tau=\frac{\lambda R_1}{k}$ at a fixed Z-position is defined as

$$\hat{Q}=\frac{1}{\tau}\int_0^{\tau} Qd\tau. \tag{17}$$

We assume that the tube length is an integral multiple of wavelength λ. Also, the pressure difference across the ends of the tube is assumed to be a constant. Therefore, the flow which is unsteady in laboratory frame $(R,0,Z)$ becomes steady in the wave frame $(r,0,z)$. The transformation between these two frames is given by

$$u=U,\qquad w=W-\frac{k}{R_1},\qquad r=R,\qquad \text{and}\qquad z=Z-\frac{k}{R_1}t. \tag{18}$$

It is convenient to write the above equations in an appropriate dimensionless form. This can be done in a number of ways depending primarily on the choice of the characteristic length, time, and mass. Consider the following dimensionless forms depending on the characteristic length R_1, λ and the characteristic mass M. The other dimensionless quantities are given by

$$\overline{r}=\frac{r}{R_1},\overline{z}=\frac{z}{\lambda},\overline{u}=\frac{uR_1}{k\delta},\overline{w}=\frac{wR_1}{k},\overline{h_1}=\frac{h_1}{R_1},\delta=\frac{R_1}{\lambda}$$
$$\overline{S}=\frac{SR_1^2}{\eta k},\overline{z_0}=\frac{z_0}{\lambda},\overline{L}=\frac{L}{\lambda},\overline{h}=\frac{h}{R_1},\overline{d}=\frac{d}{\lambda},\overline{R(z)}=\frac{R(z)}{R_1},$$
$$\overline{\Pi}=\frac{\Pi R_1^3}{\eta\lambda k},\overline{T}=\frac{T}{\beta R_1},\overline{C}=\frac{C}{\Delta C},\overline{p}=\frac{p}{R_1^2},\text{and}\overline{q}=\frac{q}{2\pi R_1 k}, \tag{19}$$

where q is the volume flow rate in the moving coordinate system.
Consider another dimensionless parameter: $b^*=\frac{b_1}{a_1kR_1^2}$ is the sisko fluid parameter, P_r=$\frac{a_1}{\rho k}$ is the Prandtl number, ν=$\frac{\mu}{\rho}$ is the kinematic viscosity, β is the adverse temperature gradient, ε=a/R_1 is the amplitude ratio, E_c=$\frac{k^2}{R_1^3c_p}$ is the Eckert number, $B_r=P_rE_c$ is the Brickmann number, $S_c=\frac{k}{D}$ is the Schmidt number, $S_r=\frac{DK_T\beta R_1}{kT_m}\Delta C$ is the Soret number and $\gamma_1=\frac{\gamma a_1}{R_1}$ is Kudsen number or non-dimensional slip parameter. Also, $\theta_1^*=\frac{\theta_1}{\beta R_1}$ and $C_1^*=\frac{C_1}{\Delta C}$. The bars mark refer to the dimensionless quantities. From now on, these will be omitted for simplicity.
The dimensionless effective radius of the tube $R(z)$ becomes:

$$R(z)=\begin{cases}1-m(z+L) & L<z<-z_0,\\ 1-m(z+L)-\frac{H}{2}[1+\cos\frac{\pi z}{z_0}] & -z_0\le z\le z_0,\\ 1-m(z+L) & z_0<z<d,\end{cases} \tag{20}$$

Assuming that the radial velocity u is very small in comparison with the axial one w. Also, the variation in the z-direction is smaller than that in the radial one. Therefore, we may assume that $u<<w$ and $\frac{\partial w}{\partial z}<<\frac{\partial w}{\partial r}$. Also, it follows that the terms $\frac{\partial u}{\partial r},\frac{\partial^2 u}{\partial r^2},\frac{\partial^2 u}{\partial z^2}$ may be ignored [12]. Furthermore, the assumption of long wave length approximation $\delta<<1$ can be considered. Therefore, the terms of order δ and higher may be neglected. So, The dimensionless governing Eqs. (11)-(16) may be reduced to as following:
r-component:

$$\frac{\partial \Pi}{\partial r}=0\qquad , \tag{21}$$

and z-component:

$$\frac{d\Pi}{dz}=\frac{1}{r}\frac{\partial}{\partial r}\left(r[\frac{\partial w}{\partial r}+b^*(\frac{\partial w}{\partial r})^n]\right)-\frac{w}{p}, \quad (22)$$

$$\frac{1}{r}\frac{\partial}{\partial r}\left(r\frac{\partial T}{\partial r}\right)+B_r\left((\frac{\partial w}{\partial r})^2+b^*(\frac{\partial w}{\partial r})^{n+1}\right)=0, \quad (23)$$

$$\frac{1}{r}\frac{\partial}{\partial r}\left(r\frac{\partial C}{\partial r}\right)+S_rS_c\frac{1}{r}\frac{\partial}{\partial r}\left(r\frac{\partial T}{\partial r}\right)=0 \quad (24)$$

The dimensionless volume flow rate in the moving coordinate system become:

$$q=\int_0^{r_2} wrdr, \quad (25)$$

The dimensionless boundary conditions (9) and (10) are then become

$$u=2\pi\varepsilon\sin 2\pi z, w=-1-\gamma_1\left(\frac{\partial w}{\partial r}+b^*(\frac{\partial w}{\partial r})^n\right), T=\theta_1^*,$$
$$C=C_1^* \quad at \quad r=r_2=R(z)+h_1, \quad (26)$$

$$u=0,\frac{\partial w}{\partial r}=0,\frac{\partial T}{\partial r}=0,\frac{\partial C}{\partial r}=0 \quad at \quad r=0, \quad (27)$$

and

$$h_1=\varepsilon\cos 2\pi z. \quad (28)$$

Now, the system of Eqs. (17) and (21)-(25) are nonlinear partial differential equations. They are difficult to be solved exactly. Therefore, we are forced to consider an approximate solution by using a perturbation technique. This technique is considered in the following section.

3 An approximation solution

The following perturbation technique depends mainly on considering the small parameter of Sisko Fluid b^*. To solve the nonlinear system of Eqs. (17) and (21)-(25) under the appropriate boundary conditions as given by Eq. (26) and (27), we shall assume that any physical quantity, such as w, Π, T, C, q and $\hat{Q}$ may be represented as:

$$\xi=\xi_0+b^*\xi_1+\ldots\ldots, \quad (29)$$

where ξ_0 is the undisturbed quantity and ξ_1 is the first perturbed one.

Substituting from Eq. (29) into the system of Eqs. (17) and (21)-(25) and collect the terms of like powers of b^*. This procedure yields zero and first order systems of partial differential equations with the corresponding boundary conditions. Because of the complexity in treating these orders, we shall study the solutions in case of small intestine or artery, in accordance with the physical meaning of the length of the diameters of small arteries. Therefore, we may assume that $r<<1$. Through the following subsections, we shall consider these orders:

3.1 The zero-order system

In the absence of the sisko fluid parameterb^*, the fluid becomes a Newtonian one. Therefore, the zero-order system resulted in without any non-Newtonian parameters as follows:

r-component:

$$\frac{\partial\Pi_0}{\partial r}=0, \quad (30)$$

equation (30) decides that Π_0 is a function on z only.

z-component:

$$\frac{d\Pi_0}{dz}=\frac{1}{r}\frac{\partial}{\partial r}\left(r\frac{\partial w_0}{\partial r}\right)-\frac{w_0}{p}, \quad (31)$$

$$\frac{1}{r}\frac{\partial}{\partial r}\left(r\frac{\partial T_0}{\partial r}\right)+B_r\left(\frac{\partial w_0}{\partial r}\right)^2=0, \quad (32)$$

$$\frac{1}{r}\frac{\partial}{\partial r}\left(r\frac{\partial C_0}{\partial r}\right)+S_rS_c\frac{1}{r}\frac{\partial}{\partial r}\left(r\frac{\partial T_0}{\partial r}\right)=0. \quad (33)$$

$$q_0=\int_0^{r_2} w_0rdr, \quad (34)$$

$$\hat{Q}_0=\frac{1}{\tau}\int_0^{\tau} Q_0d\tau. \quad (35)$$

In accordance with the boundary conditions:

$$u_0=2\pi\varepsilon\sin 2\pi z,\ w_0=-1-\gamma_1\left(\frac{\partial w_0}{\partial r}\right),$$
$$T_0=\theta_1^*, \quad C_0=C_1^* \ at\ r=r_2=R(z)+h_1, \quad (36)$$

$$u_0=0,\frac{\partial w_0}{\partial r}=0,\frac{\partial T_0}{\partial r}=0, \text{ and } \frac{\partial C_0}{\partial r}=0 at r=0. \quad (37)$$

The solutions of Eqs. (31)-(35) with the boundary conditions (36) and (37) are:

$$Q_0=q_0+\frac{r_2^2}{2}, \quad (38)$$

$$\hat{Q}_0=q_0+\frac{1}{2}\left([R(z)]^2+\frac{\varepsilon^2}{2}\right). \quad (39)$$

$$G_0(z)=-\frac{4+2\frac{\gamma_1 r_2(z)}{p}}{\gamma_1(r_2(z))^3}\left(\hat{Q}_0-\frac{1}{2}\left([R(z)]^2+\frac{\varepsilon^2}{2}\right)+\frac{(r_2(z))^2}{2+\frac{\gamma_1 r_2(z)}{p}}\right), \quad (40)$$

$$w_0(r,z)=d_1(z)-pG_0(z), \quad (41)$$

$$T_0(r,z)=d_2(z)r^4+d_3(z), \quad (42)$$

and

$$C_0(r,z)=d_4(z)r^4+d_5(z), \quad (43)$$

where $G_0(z)=\frac{d\Pi_0}{dz}$ and d_1, d_2,.....,d_5 are given in the appendix.

3.2 The first-order system

The zero-order solutions obtained in the previous subsection will be combined through the first-order governed system to obtain non-homogeneous set of linear partial differential equations. This procedure will be outlined as follows:
r-component:

$$\frac{\partial \Pi_1}{\partial r} = 0 \quad , \tag{44}$$

As before, eq. (44) indicates that Π_1 is a function on z only.
z-component:

$$\frac{d\Pi_1}{dz} = \frac{1}{r}\frac{\partial}{\partial r}\left(r[\frac{\partial w_1}{\partial r} + (\frac{\partial w_0}{\partial r})^n]\right) - \frac{w_1}{p}, \tag{45}$$

$$\frac{1}{r}\frac{\partial}{\partial r}\left(r\frac{\partial T_1}{\partial r}\right) + B_r\left(2\frac{\partial w_0}{\partial r}\frac{\partial w_1}{\partial r} + (\frac{\partial w_0}{\partial r})^{n+1}\right) = 0, \tag{46}$$

$$\frac{1}{r}\frac{\partial}{\partial r}\left(r\frac{\partial C_1}{\partial r}\right) + S_r S_c \frac{1}{r}\frac{\partial}{\partial r}\left(r\frac{\partial T_1}{\partial r}\right) = 0 \tag{47}$$

$$q_1 = \int_0^{r_2} w_1 r dr, \tag{48}$$

$$\hat{Q_1} = \frac{1}{\tau}\int_0^{\tau} Q_1 d\tau. \tag{49}$$

in accordance with the appropriate boundary conditions:

$$\begin{aligned} &u_1 = 0, \qquad w_1 = -\gamma_1\left(\frac{\partial w_1}{\partial r} + (\frac{\partial w_1}{\partial r})^n\right), \qquad T_1 = 0, \\ &C_1 = 0 \qquad\quad at \qquad r = r_2 = R(z) + h_1, \end{aligned} \tag{50}$$

$$u_1 = 0, \frac{\partial w_1}{\partial r} = 0, \frac{\partial T_1}{\partial r} = 0, \text{ and } \frac{\partial C_1}{\partial r} = 0 \; at \; r = 0. \tag{51}$$

The solutions of Eqs. (45)-(49) with the boundary conditions (50) and (51) are:

$$Q_1 = q_1 + \frac{r_2^2}{2}, \tag{52}$$

$$\hat{Q_1} = q_1 + \frac{1}{2}\left([R(z)]^2 + \frac{\varepsilon^2}{2}\right). \tag{53}$$

$$\begin{aligned} G_1(z) = & \frac{1}{\frac{r_2^6}{288}(7-24\ln\frac{r_2}{\sqrt{p}}) - \frac{r_2^6}{32}(1-8\ln\frac{r_2}{\sqrt{p}}) + \frac{\gamma_1 r_2^5}{8}(1+8\ln\frac{r_2}{\sqrt{p}})} \\ & [\hat{Q_1} - \frac{1}{2}([R(z)]^2 + \frac{\varepsilon^2}{2}) - \frac{r_2^2}{2}(\frac{d_1(z)}{2p})^n(2\gamma_1 r_2^{n+2}(\frac{1}{n+3} + 2\ln\frac{r_2}{\sqrt{p}}) \\ & + \gamma_1 r_2^n + 2\frac{r_2^{n+3}}{n+3}(\frac{1}{n+3} - 2\ln\frac{r_2}{\sqrt{p}})) - 2(\frac{d_1(z)}{2p})^n\frac{r_2^{n+4}}{(n+3)^2(n+4)^2} \\ & (10+3n-2(3+n)(4+n)\ln\frac{r_2}{\sqrt{p}}))], \end{aligned} \tag{54}$$

$$\begin{aligned} w_1(r,z) = \; & d_6(z) + G_1(z)\frac{r_2^4}{16}(1-8\ln\frac{r_2}{\sqrt{p}}) \\ & + 2(\frac{d_1(z)}{2p})^n\frac{r_2^{n+3}}{n+3}(\frac{1}{n+3} - 2\ln\frac{r_2}{\sqrt{p}}), \end{aligned} \tag{55}$$

$$\begin{aligned} T_1(r,z) = \; & B_r(\frac{d_1(z)G_1(z)r^5}{500p}(-11+40\ln\frac{r_2}{\sqrt{p}}) \\ & + (\frac{d_1(z)}{2p})^{n+1}\frac{r_2^{n+4}}{(n+3)(n+4)^3} \\ & \times(-8-3n+2(3+n)(4+n)\ln\frac{r_2}{\sqrt{p}}) \\ & - (\frac{d_1(z)}{2p})^{n+1}\frac{r_2^{n+2}}{(n+2)^2}) + d_7(z), \end{aligned} \tag{56}$$

$$\begin{aligned} C_1(r,z) = \; & -B_r S_r S_c(\frac{d_1(z)G_1(z)r^5}{500p}(-11+40\ln\frac{r_2}{\sqrt{p}}) \\ & + (\frac{d_1(z)}{2p})^{n+1}\frac{r_2^{n+4}}{(n+3)(n+4)^3} \\ & \times(-8-3n+2(3+n)(4+n)\ln\frac{r_2}{\sqrt{p}}) \\ & - (\frac{d_1(z)}{2p})^{n+1}\frac{r_2^{n+2}}{(n+2)^2}) + d_8(z), \end{aligned} \tag{57}$$

where $G_1(z) = \frac{d\Pi_1}{dz}$ and d_6, d_7 and d_5 are given in the appendix. From Eqs. (40) and (54) the expression for the pressure gradient take the following form:

$$\begin{aligned} & G(z) = \\ & -\frac{4+2\frac{\gamma_1 r_2(z)}{p}}{\gamma_1(r_2(z))^3}\left(\hat{Q_0} - \frac{1}{2}\left([R(z)]^2 + \frac{\varepsilon^2}{2}\right) + \frac{(r_2(z))^2}{2+\frac{\gamma_1 r_2(z)}{p}}\right) + b^* \\ & \times(\frac{1}{\frac{r_2^6}{288}(7-24\ln\frac{r_2}{\sqrt{p}}) - \frac{r_2^6}{32}(1-8\ln\frac{r_2}{\sqrt{p}}) + \frac{\gamma_1 r_2^5}{8}(1+8\ln\frac{r_2}{\sqrt{p}})} \\ & [\hat{Q_1} - \frac{1}{2}([R(z)]^2 + \frac{\varepsilon^2}{2}) \\ & - \frac{r_2^2}{2}(\frac{d_1(z)}{2p})^n(2\gamma_1 r_2^{n+2}(\frac{1}{n+3} + 2\ln\frac{r_2}{\sqrt{p}}) \\ & + \gamma_1 r_2^n + 2\frac{r_2^{n+3}}{n+3}(\frac{1}{n+3} - 2\ln\frac{r_2}{\sqrt{p}})) \\ & - 2(\frac{d_1(z)}{2p})^n\frac{r_2^{n+4}}{(n+3)^2(n+4)^2} \\ & (10+3n-2(3+n)(4+n)\ln\frac{r_2}{\sqrt{p}}))]), \end{aligned} \tag{58}$$

where $G(z) = \frac{d\Pi}{dz}$. From Eqs. (41) and (55) the expression for the axial velocity component take the following form:

$$\begin{aligned} w(r,z) = \; & (d_1(z) - pG_0(z)) + b^*(d_6(z) \\ & + G_1(z)\frac{r_2^4}{16}(1-8\ln\frac{r_2}{\sqrt{p}}) + 2(\frac{d_1(z)}{2p})^n\frac{r_2^{n+3}}{n+3} \\ & \times(\frac{1}{n+3} - 2\ln\frac{r_2}{\sqrt{p}})). \end{aligned} \tag{59}$$

The pressure rise ΔP and the friction force ΔF (at the wall), in the tube of length L, in their non -dimensional forms, are given by

$$\Delta P = \int_0^L G(z)dz = \int_0^{d_0} G(z)dz + \int_{d_0}^{d_0+L_0} G(z)dz + \int_{d_0+L_0}^{L} G(z)dz, \quad (60)$$

$$\Delta F = \int_0^L r_2^2(-G(z))dz = \int_0^{d_0} r_2^2(-G(z))dz + \int_{d_0}^{d_0+L_0} r_2^2(-G(z))dz + \int_{d_0+L_0}^{L} r_2^2(-G(z))dz, \quad (61)$$

Because of the complexity in evaluating these integrations, the value of them are computed numerically. I think that our problem deals with non-Newtonian Sisko fluid. Also, the flow streaming through the porous medium with slip condition. Furthermore, peristaltic motion with mild stenosis through tapered artery are considered. Moreover, the effects of chemical reaction with heat transfer rea taken into account. Therefore, this problem can be considered as a general problem. In case of ignoring these consideration (b^*, γ_1, h and ϕ tends to zero and p tends to ∞), the terms of the pressure rise and friction force give the previous results obtained by Shapiro et al. [4].

4 Discussion of the results

In what follows, numerical calculations will be made. It is convenient to classify these calculations into two categories, as follows:

4.1 Pumping characteristics

In order to identify the quantitative effects of various parameters on the obtained distributions of the axial velocity w, temperature T, concentration C, pressure rise ΔP and friction force, the mathematical software (Mathematica) is used. Some important results are graphically displayed in Figures 2-8 as follows.

Figures 2-$\mathbb{A}$ describes the variation of axial velocity w versus (vs) z-axis for different values of the slip parameter γ_1. It is observed that the axial velocity increases with the increase of γ_1. It is also found that, in case of no-slip condition ($\gamma_1 = 0$), the value of the axial velocity is lower than that in case of slip condition. Figures 2-$\mathbb{B}$ indicates the variation of axial velocity $w(z)$ for different values of permeability parameter p. It is showed that the axial velocity decreases with the increase of p. Figures 2-$\mathbb{C}$ shows the variation of axial velocity $w(z)$ for different values of power index n. It is indicated that, when n is an integer, the axial velocity decreases with the increase of n. Furthermore, it is observed that in case of Newtonian behavior $n = 1$, the values of the axial velocity is greater than those in case of shear thinning behavior $n < 1$ and also for shear thickening one $n > 1$. Figures 2-$\mathbb{D}$ indicates the variation of axial velocity $w(z)$ for different values of maximum height of stenosis h. It is observed that the domain of the maximum height of stenosis h becomes ($0.01 \leq z \leq 0.71$), the axial velocity decreases with the increase of h. Meanwhile, at the complementary of this domain, the curves of this velocity are coincide to each others. It is also found that, in case of no-stenosis ($h = 0$), the values of the axial velocity is greater than that in case of stenosis. Therefore, for the diseases of blood clot, the existence of the clots at the artery straitens the blood flow and leads to a harmful effects for the body organs [10].

Figure 3-$\mathbb{A}$ indicates the variation of axial velocity w vs radial distance r for different values of the taper angle ϕ. The importance of the effect of vessel tapering with the shape of stenosis deserves special attention. Also, the tapering has a significant aspect arterial system [12]. Therefore, we are interested in studying the flow through a tapered tube with stenosis. It is observed that in case of the diverging tapered artery $\phi = 0.05(> 0)$, the values of the axial velocity are greater than those in case of the non tapered artery $\phi = 0$ and the convergent tapered one $\phi = -0.05(< 0)$. Figures 3-$\mathbb{B}$ shows the variation of axial velocity $w(r)$ for different values of the Sisko parameter b^*. It indicates that the ratio of a power-low part to a viscous part in a Sisko fluid if ($n \neq 1$). The case of ($n \neq 1$, $b_1^* = 0$) denotes a viscous Newtonian fluid. Meanwhile, the case of ($b^* \to \infty$) describes a purely power-low model [24]. It is noted that the axial velocity decreases with the increase of b^*. Furthermore, the transmission of axial velocity curves through a Newtonian fluid ($b^* = 0$) is substantially greater than that in case of a Sisko fluid. Furthermore, the influence of this parameter is in agreement with the previous work of Mekheimer and El Kot [24]. Figure 3-$\mathbb{C}$ indicates the variation of axial velocity $w(r)$ for different values of the flow rate Q. It is observed that the axial velocity increases by the increasing of Q.

The variation of temperature profile $T(z)$ for different values of Brickmann number B_r is shown in figure 4-$\mathbb{A}$. It

is observed that the temperature increases with the increase of B_r. Figure 4-$\mathbb{B}$ describes the variation of temperature $T(z)$ for different values of the Sisko parameter b^*. It is noted that the temperature increases with the increase of b^*. Moreover, the transmission of the temperature curves through a Sisko fluid is substantially greater than that through a Newtonian fluid ($b^* = 0$) . Figure 5-$\mathbb{A}$ describes the variation of temperature $T(r)$ for different values of permeability parameter p. It is observed that the temperature decreases with the increase of p. The variation of temperature profile $T(r)$ for different values of power index n is described in figure 5-$\mathbb{B}$. It is indicated that in case of Newtonian behavior $n = 1$, the values of the temperature is lower than those in case of shear thinning behavior $n < 1$ and also for shear thickening one $n > 1$. Figure 6-$\mathbb{A}$ indicates the variation of concentration C vs z-axis for different values of permeability parameter p. It is cleared that the concentration increases with the increase of p. Figure 6-$\mathbb{B}$ describes the variation of concentration C vs z-axis for different values of Soret number S_r. It is noted that the concentration decreases with the increase of S_r.

The pressure rise ΔP is plotted vs the mean flow rate for different values of Sisko parameter b^* in figure 7-$\mathbb{A}$. It is observed that with an increase in b^*, the pressure rise increase. Also, it is found that the transmission of the curves through a Sisko fluid ($b^* \neq 0$) is greater than that through a Newtonian fluid ($b^* = 0$). Furthermore, the peristaltic pumping is defined at the region when ($\Delta P > 0$ and $Q > 0$) (pumping region). It os noticed that the peristaltic pumping region becomes wider as the Sisko parameter b^* increases. Figure 7-$\mathbb{B}$ describes the variation of pressure rise vs the mean flow rate for different values of taper angle ϕ. It is observed that for a shear thickening fluid ($n = 2$), there exist a critical flow rate Q_c at ($Q = 0.02$) approximately. As the domain of the Q becomes ($-0.1 \leq Q \leq Q_c$), in case of the diverging tapered artery $\phi = 0.05(> 0)$, the values of the pressure rise are greater than those in case of the non tapered artery $\phi = 0$ and the convergent tapered one $\phi = -0.05(< 0)$. Meanwhile, the inverse occurs at the complementary of this domain. Furthermore, it is noticed that, for a shear thinning fluid ($n = 0.5$), in case of converging tapering artery $\phi = -0.05(< 0)$, the values of pressure rise are greater than those in case of the non tapered one $\phi = 0$ and the diverging tapered one $\phi = 0.05(> 0)$. Therefore, the blood can flow freely through diverging arteries, which have less effect of pressure drop [24]. The pressure rise is plotted vs the mean flow rate for different values of permeability parameter p in figure 7-$\mathbb{C}$. It is observed that the pressure rise decrease with the increase of p. Figure 7-$\mathbb{D}$ shows the variation of pressure rise vs the mean flow rate for different values of slip parameter γ_1. It is found a critical flow rate Q_c at ($Q = 0.03$) approximately. As the domain of the Q becomes ($-0.1 \leq Q \leq Q_c$), the pressure rise decrease with the increase of γ_1. Meanwhile, the inverse occurs at the complementary of this domain. From the pervious figures, it is found that the increase in mean flow rate decreases the pressure rise. Therefore, the maximum flow rate is achieved at zero pressure rise. Also, the maximum pressure rise occurs at zero flow rate. Finally, the relation between pressure rise and mean flow rate is linear.

The friction force at the wall ΔF is plotted vs the mean flow rate for different values of permeability parameter **p** in figure 8-$\mathbb{A}$. It is observed that the friction force increase with the increase of p. Figure 8-$\mathbb{B}$ shows the variation of friction force vs the mean flow rate for different values of slip parameter γ_1. It found a critical flow rate Q_c at ($Q = 0.01$) approximately. As the domain of the Q becomes ($-0.1 \leq Q \leq Q_c$), the friction force increase with the increase of γ_1. Meanwhile, the inverse occurs at the complementary of this domain. It is noticed that, from these paragraph and previous paragraph, the friction force has the opposite behavior compared to the pressure rise.

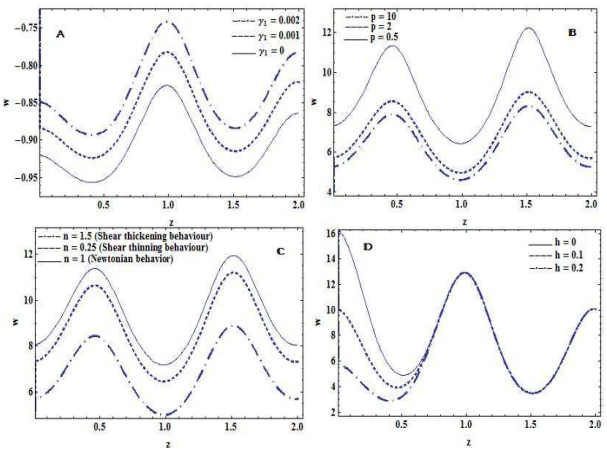

Fig. 2: indicates the variation of the axial velocity w with z-axis for different values of γ_1, p, n and h.

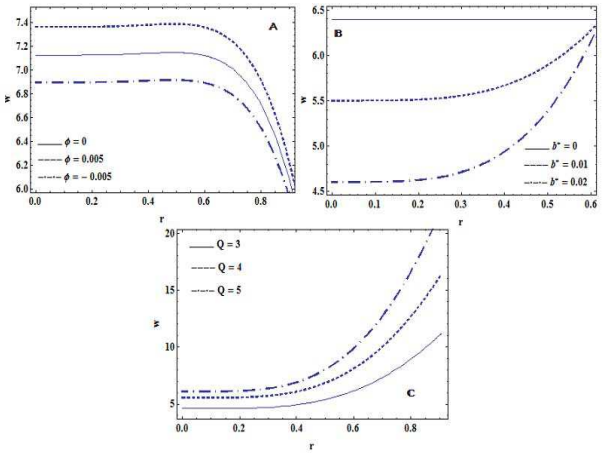

Fig. 3: indicates the variation of the axial velocity w with r-axis for different values of ϕ, b^* and Q.

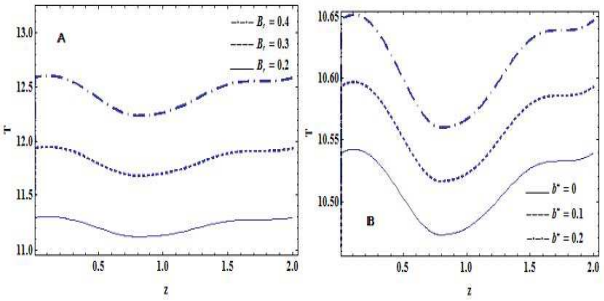

Fig. 4: indicates the variation of the temperature distribution T with z-axis for different values of B_r and b^*.

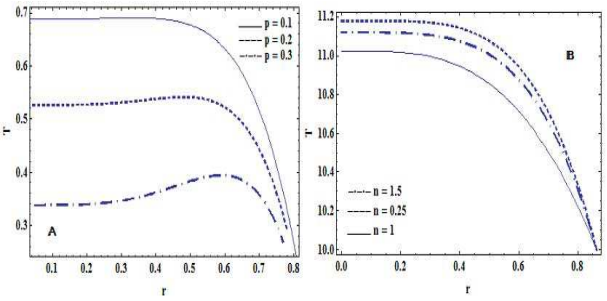

Fig. 5: indicates the variation of the temperature distribution T with r-axis for different values of p and n.

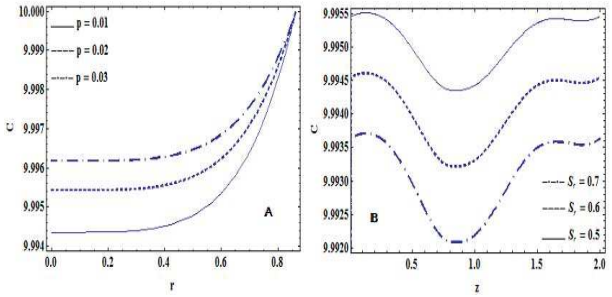

Fig. 6: indicates the variation of the concentration T for different values of p and S_r.

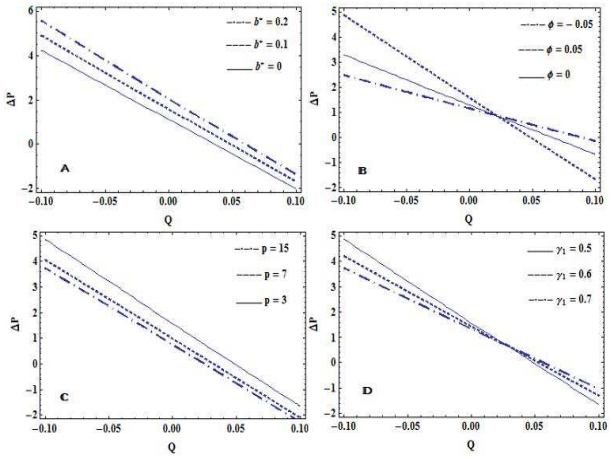

Fig. 7: indicates the variation of pressure rise ΔP vs mean flow rate for different values of b^*, ϕ, p and γ_1.

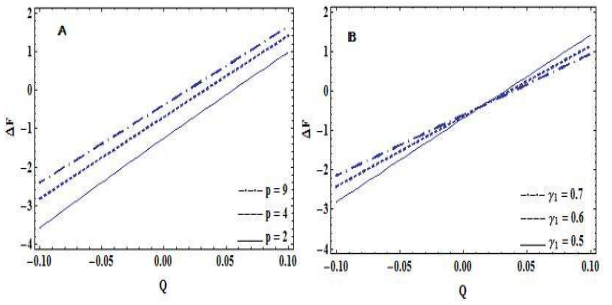

Fig. 8: indicates the variation of friction force ΔF vs mean flow rate for different values of p and γ_1.

4.2 Trapping

In addition to the pumping phenomenon, trapping is considered as another motivating physical phenomenon in peristaltic motion. As the walls are stationary, trapping phenomenon may be anticipated that the streamlines have a shape similar to the walls. However, in the wave frame,

some streamlines under specific conditions may be separated to enclose a bolus of fluid particles in closed streamlines. Therefore, the structure of an internally circulating bolus of the fluid by closed stream lines is defined as a trapping. Furthermore, this trapped bolus is moved forward along with the speed of the peristaltic wave. Also, bolus is defined as a volume of fluid bounded by closed streamlines. In addition, the trapping phenomenon has been discussed by many researchers, such that Shapiro [4] and Jaffrin [32]. The following figures illustrate the stream lines graphes for different values of several parameters.

The effect of the Sisko parameter b^* on trapping is illustrated in figure 9. It is observed that the trapped bolus increases in size by the increasing of the Sisko parameter b^*. The effect of the slip parameter γ_1 is illustrated in figure 10. It is observed that the size of trapping bolus increases by the increasing of γ_1. The effects of the maximum height of stenosis h on the trapping are displayed in figures 11. It is observed that the bolus increases in size by the increasing of h. The effects of the permeability parameter p on the trapping are displayed in figures 12. It is observed that the bolus decreases in size by the increasing of p.

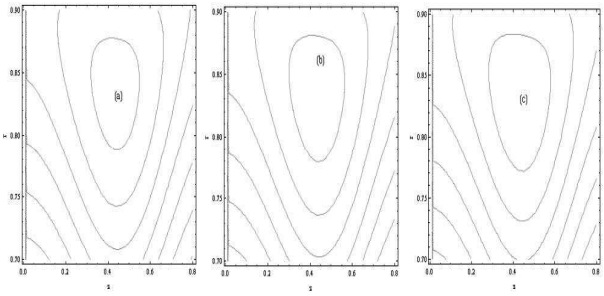

Fig. 9: Streamlines for different values of Sisko parameter b^*.

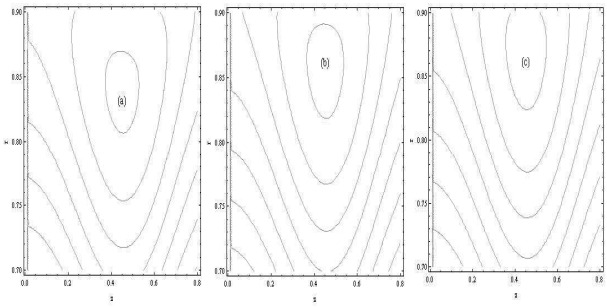

Fig. 10: Streamlines for different values of slip parameter γ_1.

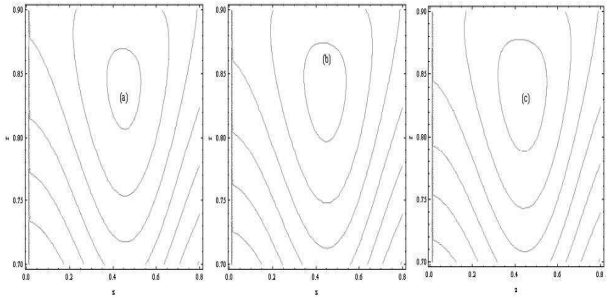

Fig. 11: Streamlines for different values of maximum height of stenosis h.

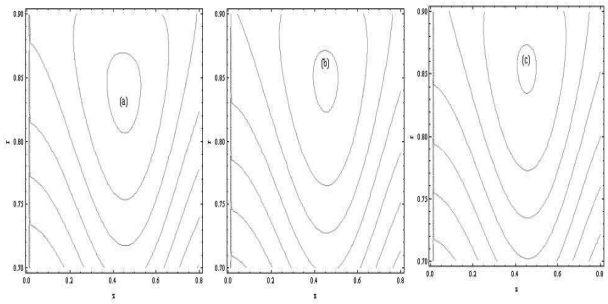

Fig. 12: Streamlines for different values of permeability parameter **p**.

5 Conclusions

In this study we have presented a theoretical approach to investigate the effects of heat and chemical reactions on peristaltic transport of blood flow. The flow is streaming through a tapered artery with mild stenosis. The blood is represented by a Sisko model. Furthermore, the influences of slip condition and porous medium are studied. The governing equations of motion, energy and concentration are analytically solved by using the long wavelength and low Reynolds number approximations. These equations are treated in accordance with the appropriate boundary conditions. The analytical solutions depend on a perturbation method. This technique considered a small Sisko fluid parameter b^*. The distributions of velocity, stream function, temperature and concentration are obtained up to the first order. The

expressions for pressure rise and friction force are obtained in terms of dimensionless flow rate Q by using the numerical integration. The numerical calculations are adopted to obtain the effects of several parameters, such as the slip parameter γ_1, permeability parameter p, the taper angle, Brickmann number B_r, Soret number S_r and the maximum height of stenosis h, on the above distributions. Trapping phenomena is also discussed.
The concluding remarks may be drawn as follows:

–Pumping characteristics

1.The axial velocity increases with the increase of γ_1 and by the decrease of both p and b^*.
2.As the domain of the maximum height of stenosis h becomes $(0.01 \leq z \leq 0.71)$, the axial velocity decreases with the increase of h. Meanwhile, at the complementary of this domain, the curves of this velocity are coincide to each others.
3.The temperature increases with the increase of B_r.
4.The concentration decreases with the increase of S_r.
5.As the domain of the Q becomes $(-0.1 \leq Q \leq 0.02)$, in case of the diverging tapered artery $\phi = 0.05(> 0)$, the values of the pressure rise are greater than those in case of the non tapered artery $\phi = 0$ and the convergent tapered one $\phi = -0.05(< 0)$. Meanwhile, the inverse occurs at the complementary of this domain.
6.The increase in mean flow rate decreases the pressure rise. Therefore, the maximum flow rate is achieved at zero pressure rise. Also, the maximum pressure rise occurs at zero flow rate.
7.There exist a critical flow rate Q_c at $(Q = 0.01)$ approximately. As the domain of the Q becomes $(-0.1 \leq Q \leq Q_c)$, the friction force increases with the increase of γ_1. Meanwhile, the inverse occurs at the complementary of this domain.
8.The friction force has the opposite behavior compared to the pressure rise.

–Trapping

1.The size of the trapped bolus decreases with the increasing of permeability parameter p.
2.The size of the trapped bolus increases with the increasing of Sisko parameter b^*, slip parameter γ_1 and maximum height of stenosis h.

To the best of our knowledge, This study is very important in the field of fluid mechanics because it have many applications in many scientific fields such as medicine, medical industrial and others.

Caption of figures

–Figure 2-$\mathbb{A}$ is prepared for various values of the parameters: $L = 1$, $d = 2$, $z_0 = 0.8$, $Q = 3$, $\mathbf{p} = 0.01$, $b^* = 0.1$, $\varepsilon = 0.1$, $n = 0.5$, $\phi = 0.05$, $h = 0.2$ and $(\gamma_1 = 0, 0.001, 0.002)$.
–Figure 2-$\mathbb{B}$ is prepared for various values of the parameters: $L = 1$, $d = 2$, $z_0 = 0.8$, $Q = 3$, $\gamma_1 = 0.5$, $b^* = 0.1$, $\varepsilon = 0.1$, $n = 1.7$, $\phi = 0.05$, $h = 0.1$ and $(\mathbf{p} = 0.5, 2, 10)$.
–Figure 2-$\mathbb{C}$ is prepared for various values of the parameters: $L = 1$, $d = 2$, $z_0 = 0.8$, $Q = 3$, $\gamma_1 = 0.5$, $b^* = 0.1$, $\varepsilon = 0.1$, $\mathbf{p} = 3$, $\phi = 0.05$, $h = 0.1$ and $(n = 1, 0.25, 1.5)$.
–Figure 2-$\mathbb{D}$ is prepared for various values of the parameters: $L = 1$, $d = 2$, $z_0 = 0.8$, $Q = 3$, $\gamma_1 = 0.01$, $b^* = 0.01$, $\varepsilon = 0.1$, $\mathbf{p} = 0.01$, $\phi = 0.05$, $n = 2$ and $(h = 0, 0.1, 0.2)$.
–Figure 3-$\mathbb{A}$ is prepared for various values of the parameters: $L = 1$, $d = 2$, $z_0 = 0.8$, $Q = 3$, $\gamma_1 = 0.5$, $b^* = 0.01$, $\varepsilon = 0.1$, $\mathbf{p} = 0.01$, $n = 2$, $h = 0.1$ and $(\phi = 0, 0.005, -0.005)$.
–Figure 3-$\mathbb{B}$ is prepared for various values of the parameters: $L = 1$, $d = 2$, $z_0 = 0.8$, $Q = 3$, $\gamma_1 = 0.5$, $n = 1.7$, $\varepsilon = 0.1$, $\mathbf{p} = 3$, $\phi = 0.05$, $h = 0.1$ and $(b^* = 0, 0.01, 0.02)$.
–Figure 3-$\mathbb{C}$ is prepared for various values of the parameters: $L = 1$, $d = 2$, $z_0 = 0.8$, $n = 1.7$, $\gamma_1 = 0.5$, $b^* = 0.2$, $\varepsilon = 0.1$, $\mathbf{p} = 3$, $\phi = 0.05$, $h = 0.1$ and $(Q = 3, 4, 5)$.
–Figure 4-$\mathbb{A}$ is prepared for various values of the parameters: $L = 1$, $d = 2$, $z_0 = 0.8$, $n = 0.5$, $\gamma_1 = 0.8$, $b^* = 0.2$, $\varepsilon = 0.01$, $\mathbf{p} = 0.01$, $\phi = 0.05$, $\theta_1^* = 10$, Q=3, $h = 0.1$ and $(B_r = 0.2, 0.3, 0.4)$.
–Figure 4-$\mathbb{B}$ is prepared for various values of the parameters: $L = 1$, $d = 2$, $z_0 = 0.8$, $n = 0.5$, $\gamma_1 = 0.8$, $B_r = 0.2$, $\varepsilon = 0.01$, $\mathbf{p} = 0.01$, $\phi = 0.05$, $\theta_1^* = 10$, Q=3, $h = 0.1$ and $(b^* = 0, 0.1, 0.2)$.
–Figure 5-$\mathbb{A}$ is prepared for various values of the parameters: $L = 1$, $d = 2$, $z_0 = 0.8$, $n = 0.5$, $\gamma_1 = 0.8$, $B_r = 0.1$, $\varepsilon = 0.01$, $b^* = 0.01$, $\phi = 0.05$, $\theta_1^* = 10$, Q=3, $h = 0.1$ and $(\mathbf{p} = 0.1, 0.2, 0.3)$.
–Figure 5-$\mathbb{B}$ is prepared for various values of the parameters: $L = 1$, $d = 2$, $z_0 = 0.8$, $b^* = 0.01$, $\gamma_1 = 0.8$, $B_r = 0.1$, $\varepsilon = 0.01$, $\mathbf{p} = 0.01$, $\phi = 0.05$, $\theta_1^* = 10$, Q=3, $h = 0.1$ and $(n = 1, 0.25, 1.5)$.
–Figures 6-$\mathbb{A}$ is prepared for various values of the parameters: $L = 1$, $d = 2$, $z_0 = 0.8$, $n = 1.5$, $\gamma_1 = 0.8$, $B_r = 0.1$, $S_c = .4$, $S_r = 0.5$, $\varepsilon = 0.01$, $b^* = 0.2$,

$\phi = 0.05$, $c_1^* = 10$, Q=3, $h = 0.1$ and ($\mathbf{p} = 0.01, 0.02, 0.03$).

–Figures 6-$\mathbb{B}$ is prepared for various values of the parameters: $L = 1$, $d = 2$, $z_0 = 0.8$, $n = 1.5$, $\gamma_1 = 0.8$, $B_r = 0.1$, $S_c = .4$, $\mathbf{p} = 0.01$, $\varepsilon = 0.01$, $b^* = 0.2$, $\phi = 0.05$, $c_1^* = 10$, Q=3, $h = 0.1$ and ($S_r = 0.5, 0.6, 0.7$).

–Figure 7-$\mathbb{A}$ is prepared for various values of the parameters: $L = 1$, $d = 2$, $z_0 = 0.8$, $\mathbf{p} = 3$, $\varepsilon = 0.1$, $n = 1.5$, $\gamma_1 = 0.5$, $\phi = 0.05$, $h = 0.2$ and ($b^* = 0, 0.1, 0.2$).

–Figure 7-$\mathbb{B}$ is prepared for various values of the parameters: $L = 1$, $d = 2$, $z_0 = 0.8$, $\gamma_1 = 0.5$, $b^* = 0.1$, $\varepsilon = 0.1$, $n = 2$, $\mathbf{p} = 3$, $h = 0.1$ and ($\phi = 0, 0.05, -0.05$).

–Figure 7-$\mathbb{C}$ is prepared for various values of the parameters: $L = 1$, $d = 2$, $z_0 = 0.8$, $\gamma_1 = 0.5$, $b^* = 0.1$, $\varepsilon = 0.1$, $n = 2$, $\phi = 0.05$, $h = 0.1$ and ($\mathbf{p} = 3, 7, 15$).

–Figure 7-$\mathbb{D}$ is prepared for various values of the parameters: $L = 1$, $d = 2$, $z_0 = 0.8$, $h = 0.1$, $b^* = 0.1$, $\varepsilon = 0.1$, $\mathbf{p} = 3$, $\phi = 0.05$, $n = 2$ and ($\gamma_1 = 0.5, 0.6, 0.7$).

–Figure 8-$\mathbb{A}$ is prepared for various values of the parameters: $L = 1$, $d = 2$, $z_0 = 0.8$, $\varepsilon = 0.1$, $n = 2$, $\gamma_1 = 0.5$, $\phi = 0.05$, $b^* = 0.1$, $h = 0.1$ and ($\mathbf{p} = 2, 4, 9$).

–Figure 8-$\mathbb{B}$ is prepared for various values of the parameters: $L = 1$, $d = 2$, $z_0 = 0.8$, $\phi = 0.05$, $b^* = 0.1$, $\varepsilon = 0.1$, $n = 2$, $\mathbf{p} = 4$, $h = 0.1$ and ($\gamma_1 = 0.5, 0.6, 0.7$).

–Figure 9: Stream lines for $L = 1$, $d = 2$, $z_0 = 0.8$, $\mathbf{p} = 0.001$, $\varepsilon = 0.1$, $n = 1.7$, $\gamma_1 = 0.5$, $\phi = 0.05$, $h = 0.12$, $Q = 3$ and ($b^* = 0.2, 0.205, 0.21$).

–Figure 10: Stream lines for $L = 1$, $d = 2$, $z_0 = 0.8$, $\mathbf{p} = 0.001$, $\varepsilon = 0.1$, $n = 1.7$, $b^* = 0.2$, $\phi = 0.05$, $h = 0.1$, $Q = 3$ and ($\gamma_1 = 0.5, 0.53, 0.55$).

–Figure 12: Stream lines for $L = 1$, $d = 2$, $z_0 = 0.8$, $\mathbf{p} = 0.001$, $\varepsilon = 0.1$, $n = 1.7$, $b^* = 0.2$, $\phi = 0.05$, $\gamma_1 = 0.5$, $Q = 3$ and ($h = 0.1, 0.11, 0.12$).

–Figure 15: Stream lines for $L = 1$, $d = 2$, $z_0 = 0.8$, $\gamma_1 = 0.5$, $\varepsilon = 0.1$, $n = 1.7$, $b^* = 0.2$, $\phi = 0.05$, $h = 0.1$, $Q = 3$ and ($\mathbf{p} = 0.001, 0.0015, 0.002$).

Appendix

The constant coefficients $c_\imath$,$\imath$=1,2,....,8 are given by the following forms:

$$d_1(z) = \frac{pG_0(z)-1}{1+\frac{\gamma_1 r_2(z)}{2p}},$$

$$d_2(z) = -\frac{B_r d_1^2(z)}{64p},$$

$$d_3(z) = \theta_1^* - d_2(z) r_2^4(z),$$

$$d_4(z) = -S_r S_c d_2(z),$$

$$d_5(z) = c_1^* - d_4(z) r_2^4(z),$$

$$d_6(z) = \gamma_1 [G_1(z) r_2^3(z)(\tfrac{1}{4} + 2\ln\tfrac{r_2}{\sqrt{p}}) + 2(\tfrac{d_1(z)}{2p})^n r_2^{n+2}(\tfrac{1}{n+3} + 2\ln\tfrac{r_2}{\sqrt{p}}) + (\tfrac{d_1(z)}{2p})^n r_2^n] - \tfrac{G_1(z) r_2^4(z)}{2}(\tfrac{1}{8} - \ln\tfrac{r_2}{\sqrt{p}}) + 2(\tfrac{d_1(z)}{2p})^n \tfrac{r_2^{n+3}}{n+3}(\tfrac{1}{n+3} - 2\ln\tfrac{r_2}{\sqrt{p}}),$$

$$d_7(z) = -B_r [\tfrac{d_1(z) G_1(z) r_2^5(z)}{500p}(-11 + 40\ln\tfrac{r_2}{\sqrt{p}}) + \tfrac{4}{(n+3)(n+4)^3}(\tfrac{d_1(z)}{2p})^{n+1} r_2^{n+4} \times(-8 - 3n + 2(3+n)(4+n)\ln\tfrac{r_2}{\sqrt{p}}) - (\tfrac{d_1(z)}{2p})^{n+1} \tfrac{r_2^{n+2}}{(n+2)^2}],$$

$$d_8(z) = -S_r S_c d_7(z).$$

References

[1] Sisko A. W., The flow of lubricating greases, Indust. Engin. Chemist., 50 (1958) 1789-1792.

[2] Khan M., Abbas Q., Duru K., Magnetohydrodynamic flow of a Sisko fluid in annular pipe: A numerical study, Int. J. Numer. Meth. fluids, 62 (2010) 1169-1180.

[3] Burns J.C., Parkes T., Peristaltic motion, J. Fluid Mech., 29 (1967) 731-743.

[4] Shapiro A. H., Jaffrin M. Y., Weinberg S. L., Peristaltic pumping with long wave lengths at low Reynolds number, J. Fluid Mech., 37 (1969) 799-825.

[5] Manton M. J., Long-wave length peristaltic pumping at low Reynolds number, J. Fluid Mech., 68 (1975) 467-476.

[6] Latham T. W., Fluid motion in a peristaltic pump, MS Thesis, MIT, Cambridge, M.A., (1966).

[7] Fung Y. C., Yin F., Peristaltic waves in circular cylindrical tubes, J. Appl. Mech., 36 (1969) 579-587.

[8] Asif I. M., Chakravarty S., Mandal P. K., An unsteady peristaltic transport phenomenon of non-Newtonian fluid - A generalised approach, Appl. Math. Comput., 201 (2008) 16-34.

[9] Ang K.C., Mazumdar J.N., Mathematical modeling of three dimentional flow through an asymmetric arterial stenosis, Math. Comput. Modell., 25 (1997) 19-29.

[10] Nichols W. W., Orourke M. F., McDonald's Blood Flow in Arteries, USA by Oxford University Press, Inc., New York, (1973).

[11] Chakravarty S., Datta A., Mandal P.K., Analysis of nonlinear blood flow in a stenosed flexible artery, Int. J. Eng. Sci., 33 (1995) 1821-1837.

[12] Verma N., Parihar R. S., Mathematical model of blood flow through a tapered artery with mild stenosis and hematocrit, J. Mod. Math. Stat., 4 (2010) 38-43.

[13] Srinivas S., Kothandapani M. Peristaltic transport in an asymmetric channel with heat transfer, Int. Comm. Heat Mass Trans. 35 (2008) 514-522.

[14] Arora C. P., Heat and Mass Transfer, 2nd ed., Khanna Publishers, Delhi, (1997).

[15] Nadeem S., Akbar N. S., Influence of heat transfer on a peristaltic transport of Herschel-Bulkley fluid in a non uniform inclined tube, Commun. Nonlinear Sci. Numer. Simulat., 14 (2009) 4100-4113.

[16] Eldabe N. T. M., El-Sayed M. F., Ghaly A. Y., Sayed H. M., Mixed convective heat and mass transfer in a non Newtonian fluid at a peristaltic surface with temperature-dependent viscosity, Arch. Appl. Mech., 78 (2008) 599-624.

[17] Srinivas S., Kothandapani M., The influence of heat and mass transfer on MHD peristaltic flow through a porous space with compliant walls, Appl. Math. Comput., 213 (2009) 197-208.

[18] Alam M. S., Rahman M. M., Dufour and Soret effects on mixed convection flow past a vertical porous flat plate with variable suction, Nonlin. Analysis: Model. & Cont., 11 (2006) 3-12.

[19] Dursunkaya Z., Worek W. M., Diffusion-thermo and thermal diffusion effects in transient and steady natural convection from a vertical surface, Int. J. Heat Mass Trans., 35 (1992) 2060-2065 .

[20] Nadeem S., Akbar N. S., Influence of heat and chemical reaction on Walter's B model for blood flow through a tapered artery, J. Taiwan Inst. of Chem. Engin., 42 (2011) 67-75.

[21] Chakravarty S., Sen S., Dynamic response of heat and mass transfer in blood flow through stenosed bifurcated arteries, Korea-Aust. Rheol. J., 17 (2005) 47-54.

[22] Pandey S. K., Chaube M. K., Peristaltic transport of a visco-elastic fluid in a tube of non-uniform cross section, Math. Comput. Modell., 52 (2010) 501-514.

[23] Mandal P.K., An unsteady of non-Newtonian blood flow through tapered arteries with a stenosis, Int. J. Nonlin. Mech., 40 (2005) 151-164.

[24] Mekheimer K. S, El Kot M. A., Mathematical modelling of unsteady flow os a Sisko fluid through an anisotropically tapered elastic arteries with time variant overlapping stenosis, Appl. Math. Modell., 36 (2012) 5393-5407.

[25] Scheidegger A. E., The Physics of Flow through Porous Media, McGraw-Hill, New York, (1963).

[26] Eldabe N. T. M., Ghaly A. Y., Sayed H. M., MHD Peristaltic flow of non Newtonian fluid through a porous medium in circular cylindrical tube, Bull. Cal. Math. Soc., 99 (2007) 123-136.

[27] Mekheimer K. S., Non-linear peristaltic transport through a porous medium in an inclined planner channel, J. Porous Media, 6 (2003) 189-201.

[28] Afsar A., Khan R., Ellahi K., Vafai, Peristaltic transport of jeffrey fluid with variable viscosity through a porous medium in an asymmetric channel, Adv. Math. Phy., 2012 (2012) 1-15.

[29] Tretheway D. C., Meinhart C. D., Apperant fluid slip at hydrophobic microchannel walls, Phys. Fluids, 14 (2002) 9-12.

[30] Ebaid A., Effects of magnetic field and wall slip conditions on the peristaltic transport of a newtonian fluid in an asymmetric channel, Phys. Lett. A, 372 (2008) 4493-4499.

[31] Mekheimer K. S., Salem A. M., Zaher A. Z., Peristatcally induced MHD slip flow in a porous medium due to a surface acoustic wavy wall, J. Egypt. Math. Soc., 22 (2014) 143-151.

[32] Jaffrin M. Y., Inertia and streamline curvature effects on peristalsis pumping, Int. J. Engng. Sci., 11 (1973) 681-699.

Nabil El-dabe received the B.S. in 1970 at the Department of Mathematics in Faculty of Education, Ain Shams University, Cairo, Egypt. Also, he received another B.S. in 1972 at the Department of Mathematics in Faculty of Science, Ain Shams University. Furthermore, he received M.S. degree from Girls College, Ain Shams University, in 1975. In 1980, he received the PH.D. from Faculty of Science, Assiut University, Assiut, Egypt. From 1970 to 1974, he had been employed as demonstrator, from 1975 to 1979, he had worked as an assistant lecturer, from 1980 to 1984, he had worked as a lecturer, from 1985 to 1989 he had worked as an assistant professor and from 1990 to 2009, he had worked as a professor at Department of Mathematics, Faculty of Education, Ain Shams University. Also, from 1999 to 2005 and 2006 to 2009, he had been employed as head of the Department of Mathematics, Faculty of Education, Ain Shams Un. From 2007 to 2008, he had been employed as director for the Center of Development and Teaching Science at Ain Shams Un. From 2009 until now, he is emeritus professor in Faculty of Education, Ain Shams Un. Further, he had been employed as a head of the Department of Mathematics, Jouner College and Teachers College, Saudi Arabia from (1983 to 1988) and from (1994 to 1999). Also, he received the Amin Loutfy prize, one of the Egyptian encouragements prizes in scientific fields(1989). He was teaching most of the mathematics curriculum in Saudi Arabia, the United Arab Emirates and participating in the conferences of the Hashemite Kingdom of Jordan.

Galal Moatimid received the B.S. in 1976 at the Department of Mathematics in Faculty of Education, Ain Shams University, Cairo, Egypt. Also, he received another B.S. in 19780 at the Department of Mathematics in Faculty of Science, Ain Shams University. Furthermore, he received M.S. degree from Faculty of Science, Ain Shams University, in 1984. In 1990, he received the PH.D. in applied mathematics from Faculty of Science, Tanta University, Egypt. From 1976 to 1984, he had been employed as demonstrator , from 1985 to 1990, he had worked as an assistant teacher, from 1990 to 1995, he had worked as a lecturer, from 1995 to 2004 he had worked as an assistant professor and from 2004 to 2014, he had worked as a professor at Department of Mathematics, Faculty of Education, Ain Shams University. Also, from 2010 to 2011, he had been employed as head of the Department of Mathematics, Faculty of Education, Ain Shams Un. From 2011 to 2013, he had been employed as Vice Dean for Education and Student Affairs at Faculty of Education, Ain Shams Un. From 2015 until now, he is emeritus professor in Faculty of Education. His researches focus on EHD stability.

Mohamed Hassan received the B.S. , the M.S. and PH.D. degrees at the Department of Mathematics in Faculty of Education, Ain Shams University, Cairo, Egypt, in 1996, 2002 and 2005, respectively. He got the M.S. and Ph.D. degree in fluid mechanics. From 1997 to 2002, he had been employed as demonstrator, from 2002 to 2005, he had worked as an assistant lecturer and from 2005 to 2013, he had worked as an assistant professor at Department of Mathematics, Faculty of Education, Ain Shams University. He is currently an associate professor at the same place, where he does research on fluid mechanics.

Doaa Mostapha received the B.S., general diploma in pure and applied mathematics, special diploma in applied mathematics and the M.S. degrees at the Department of Mathematics in Faculty of Education, Ain Shams University, Cairo, Egypt, in 2007, 2008, 2009 and 2012, respectively. She got the M.S. degree in fluid mechanics about the peristaltic motion. From 2008 to 2011, she had been employed as demonstrator at Department of Mathematics, Faculty of Education, Ain Shams University. From 2012 until now, she is an assistant lecturer at the same place.